

Power load during disruption in MAST

E. Delchambre ^{a,*}, G. Counsell ^a, A. Kirk ^a, F. Lott ^b

^a EURATOM/UKAEA Fusion Association, Culham Science Centre, Abingdon, Oxfordshire OX14 3DB, UK

^b Plasma Physics Group, Blackett Laboratory, Imperial College London, London SW7 2BW, UK

Abstract

The spatial distribution and temporal behaviour of thermal energy released during disruptions is a key issue for ITER. The most critical phase of the disruption process for plasma facing components is the thermal quench which describes the rapid loss of thermal energy at, or just before, the current redistribution. Power exhaust during disruption in MAST has been investigated using an infrared (IR) camera. The spatial distribution have shown strong toroidal and radial asymmetries depending on the event triggering the collapse of the energy such as locked mode, vertical displacement event (VDE) or big sawtooth. Disruption can be characterised comparing the heat load footprint, the broadening of heat flux width and the energy released in the phase prior to the thermal quench. This paper will present results from heat load pattern and will discuss the role of plasma parameters on power load during disruption.

© 2007 Published by Elsevier B.V.

PACS: 52.55.F; 87.59.W; 52.55; 81.05.T

Keywords: MAST; Thermography; Power deposition; Disruption; ELM

1. Introduction

Expected energy fluxes to plasma facing components (PFCs) in ITER during disruption are of about tens of GW/m^2 [1] and are consequently a damaging threat for the divertor target and potentially for the first wall materials due to the broadening of the power deposition profile. On MAST a significant amount of energy (few MW/m^2) on short time scale (~ 1 ms) is ejected into the scrape-off layer (SOL) and finally to the divertor and main chamber walls. The broadening is expressed by the ratio of

the divertor power flux width at the thermal quench to that during steady state plasma conditions ($\lambda_p^{t,q}/\lambda_p^{s,s}$). A large broadening is systematically observed in MAST like in other devices [1]. In addition, it has been observed that in most MAST discharges the ratio W_r of core thermal energy at the time of the thermal quench to that during the plasma flat top is significantly less than unity due to core energy losses in the period prior to the thermal quench and the thermal energy quench is consequently smaller than that of the full plasma performance. The control of those phenomenons can be used as a signal to foresee the collapse of the plasma and prevent the damage of plasma facing components (PFCs). The control of heat load during disruption requires a good knowledge of

* Corresponding author.

E-mail address: elise.delchambre@ukaea.org.uk (E. Delchambre).

what is the energy released and where the heat flux goes in the vessel, which is why infrared thermography has been used for heat flux assessment and to better correlate heat load with edge turbulence. Indeed the dynamics of the plasma before the disruption depends on the cause of the instability that takes the plasma from its steady state condition into an unstable situation. Typical instability triggers are: thermal instability by excessive density or impurity contents and growth of MHD modes such as neoclassical tearing modes (NTMs), etc. In MAST, the deterioration of the energy confinement can appear well in advance (up to 40 ms) due to the gross of MHD instability and most of the disruptions are caused by locked mode (LM), giant sawtooth or by a loss of plasma control followed by a VDE. All those classes of disruption have been investigated.

2. Experimental set up and observations

A fast IR camera (10 kHz frequency acquisition and 4 μ s integration time) is filtered at 4.5–5 μ m to reduce surface effect disturbance [2,3] and is used to characterise heat deposition with tangential view in a windowing mode. The mid-plane wide angle views 70% of the vessel (@315 Hz with 1 ms integration time) and allows catching the toroidal and poloidal asymmetries [4]. The broadening of power width ($\lambda_p^{l,q}/\lambda_p^{s,s}$) for few analysed disruptions varies between 4.6 and 10.5. This calculation takes into account the global width in order to find out whether ITER first wall can receive a significant amount of flux. However it does not consider the broadening of fluxes which reaches the P2 cover in the inboard side and might consequently imply under-estimation. In the case of giant sawtooth, a multiple strike point structure appears (up to 12 peaks as shown in Fig. 1) due to the spiral footprint resulting from magnetic perturbation [5]. For disruption triggered by sawtooth, the global broadening can reach ~ 14 but it is a MAST characteristic due to a $q = 1$ surface closed to the edge and cannot be extrapolated to ITER. However for sawtooth triggering disruption, the multiple strike point as well as the spiral foot (Fig. 1) survives during the thermal quench and points out that thermal heat load strongly depends on magnetic configuration during the event which causes the plasma to collapse. For those events, stored energy is systematically lost in the pre-thermal quench phase like for shot #11020 (disruption triggered sawtooth) where

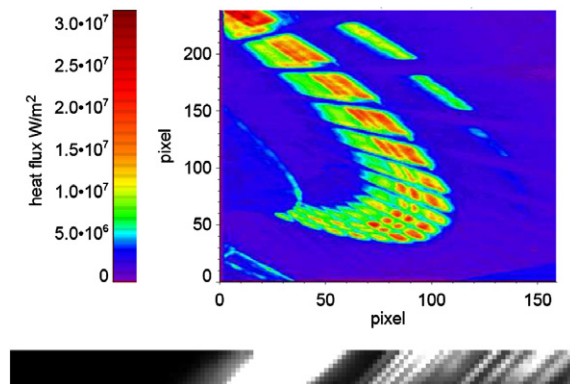


Fig. 1. (Top) Large view of disruption with a prior big sawtooth (THEODOR calculation) 68% of the core energy is lost in ~ 3 ms. (Bottom) Big sawtooth structure on the divertor for high frequency acquisition (10 kHz).

68% of the stored energy is released during ~ 3 ms in the phase prior to thermal quench.

Resonant magnetic perturbation (RMP) can drive stationary resistive tearing modes and cause unstable modes to lock as previously observed on COMPASS-D [5]. These locked perturbations leads to variations in the field-line structure. Only 2/1 neoclassical tearing modes (NTM) seems to generate LM in MAST. These modes can appear, slow down then stop rotating and a double strike appears on the divertor generated by spiral footprint. These NTM perturbations not necessarily trigger disruption however if it is the case the magnetic perturbation survive since the double strike points is still

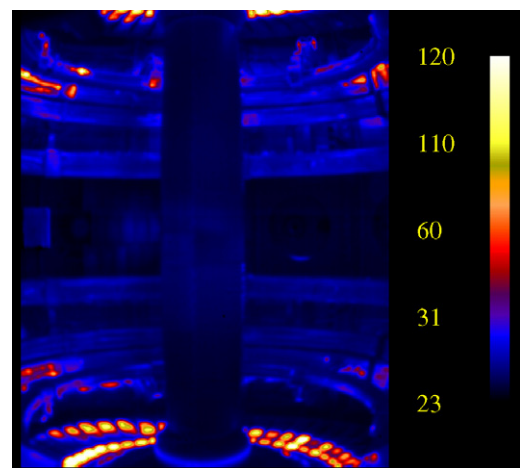


Fig. 2a. Spiral structure during disruption (TACO calculation) locked mode (#12840).

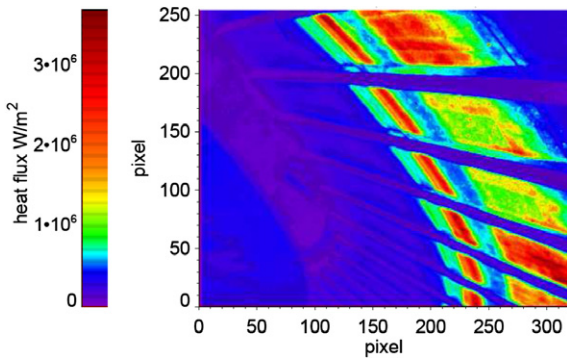


Fig. 2b. Standard locked mode disruption $\lambda_p^{1,q}/\lambda_p^{s,s} \sim 9$. Twenty percentage of the core energy is lost during thermal quench (#13409).

observed during the thermal quench and leads to a strong toroidal and poloidal asymmetries as shown in Figs. 2a and 2b. For shot #11021 (LM disruption), 20% of the stored energy is lost during ~ 20 ms prior to the disruption. The energy starts to be lost when 2/1 mode appears and during the slow down (Fig. 3) of the mode. The loss of the energy stored corresponds to the lack of good confinement and can be correlated to slow down of modes rotation at the edge. It is interesting to underline that as far as we observed, discharges

which release $\sim 100\%$ of the energy are observed with internal barrier transport (ITB) scenario when the core rotation is enhanced [6]. This effect has been observed in the case of electron ITB via counter neutral beam injection (NBI) for shots #13585 and #13589 (Fig. 4) and confirm previous result on JET [1]. Standard broadening of the heat flux is observed for disruption triggered by VDE as well as loss of energy before the thermal quench. For #11019 discharge (VDE disruption), $\lambda_p^{1,q}/\lambda_p^{s,s} \sim 9$ and of about $\sim 34\%$ of the core energy is lost in ~ 3 ms prior phase (Fig. 5). For #11018 (VDE disruption) we observed loss of energy when there is a change in the magnetic equilibrium from connected DND to disconnected DND triggers a transformation from H-mode to L-mode. Temperature on the central area of 9 tiles at three different radial position has been measured in order to observe a presumably magnetic ripple on the divertor but no clear evidence of periodic toroidal asymmetries has been seen. The toroidal field symmetry due to coil position is equal to $n = 12$ and does not corresponds to the shape observed on this view. Along each 48 tiles, there is a shadowed area due to the 4° tilt which show over heating during certain types of disruption (VDE disruption for instance) when the magnetic configuration collapses. The left over of

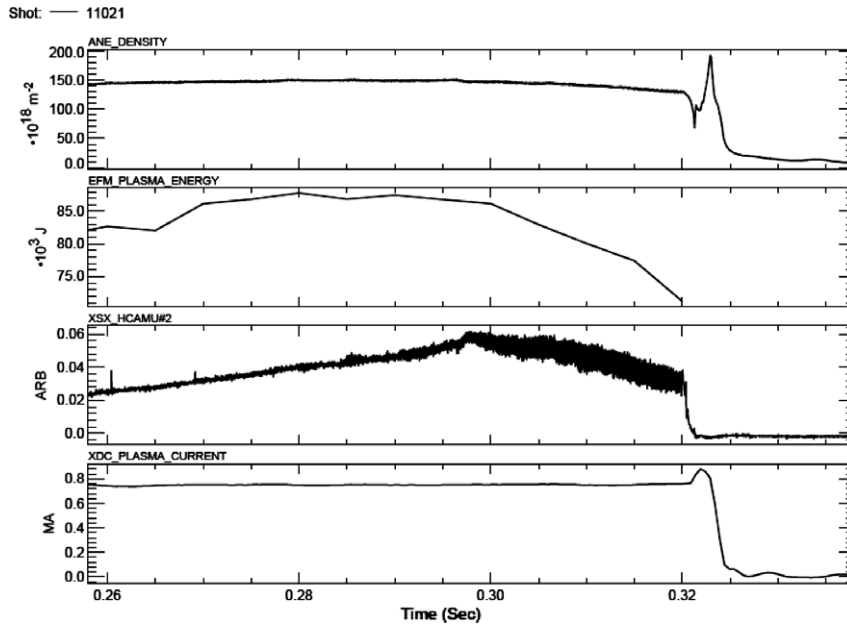


Fig. 3. Plasma parameters in the approach to a disruption. From top to bottom: density, stored energy, soft X-ray signal and plasma current. Twenty percentage of the stored energy is lost during ~ 20 ms prior to the disruption when the 2/1 mode appears and slows down (#11021).

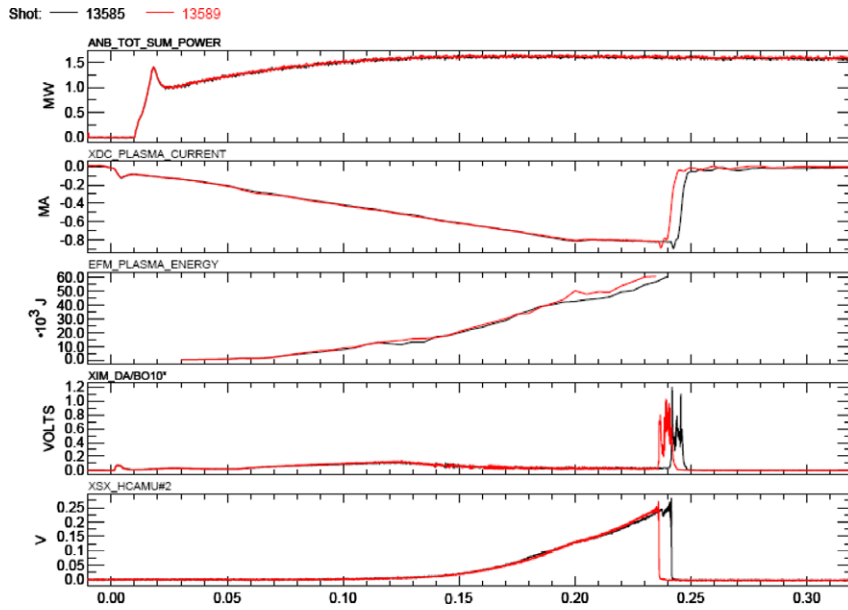


Fig. 4. Plasma parameters in the approach to a disruption. From top to bottom: total input power, neutral beam heating power, plasma current, plasma energy, D_z emission, soft X-ray signal. Hundred percentage of stored energy is released in the case of electron ITB scenario.

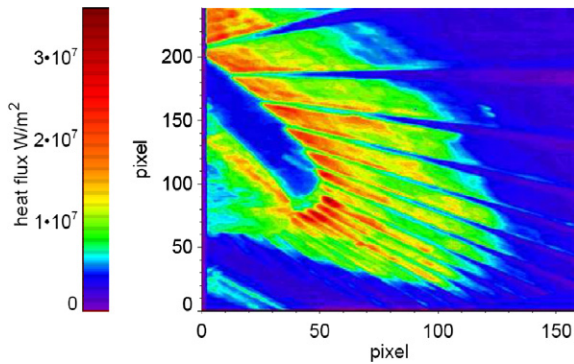


Fig. 5. VDE disruption (THEODOR calculation) $\lambda_p^{L,q}/\lambda_p^{S,S} \sim 9$. Thirty four percentage of the core energy is lost in ~ 3 ms (#11019).

dust and roughness on these less plasma exposed surface might explain the over heating of these shadowed areas during disruptions. In addition, we can pointing out that those regions are still shadowed during locked mode disruption which confirm that magnetic field are not strongly disturbed. Since spiral structure are driven for big sawtooth ($q = 1$ in the core) and no multiple structure are observed yet during ELM ($q = 1$ on the edge) on the divertor, dedicated VDE disruptions have been carried out to investigate the role of plasma parameters in the

broadening such as the position of the surface $q = 1$ and the plasma current, I_p . Identical L-mode plasma have been repeated (comparable density, stored energy and I_p) and a VDE is triggered by pushing up the plasma to $Z_{REF} = -20$ cm. Two position of $q = 1$ have been obtained modifying the I_p ramp up to delay the apparition of $q = 1$ in the plasma meanwhile IR acquisition have been made at 10 kHz and 30 kHz for fast visible camera. Three phases can be distinguished during a VDE thermal quench: increase of the heat load during the fast phase 1 ($\sim 100 \mu\text{s}$) followed by a longest phase 2 ($\sim 400 \mu\text{s}$) during which the heat load as well as the broadening increase. The phase 3 ($\sim 400 \mu\text{s}$) is characterised by the decrease of the heat load and the broadening and stripes are observed on the divertor which could be attributed to arcing on the surface during the current quench which are also observed on the fast visible camera. When $q = 1$ is at 0.13 m, the total duration of the disruption is of about ~ 0.5 ms and $\lambda_p^{L,q}/\lambda_p^{S,S} \sim 4$. For $q = 1$ at 0.25 m the total duration is ~ 0.8 ms and $\lambda_p^{L,q}/\lambda_p^{S,S} \sim 6$. In Fig. 6, heat flux profiles are compared for identical plasma discharges (energy stored and density) #15306 and #15310, with respectively $I_p = 800$ kA and $I_p = 600$ kA. The global broadening is not modified but the energy balanced between the phases 1 and 2 seems to be affected.

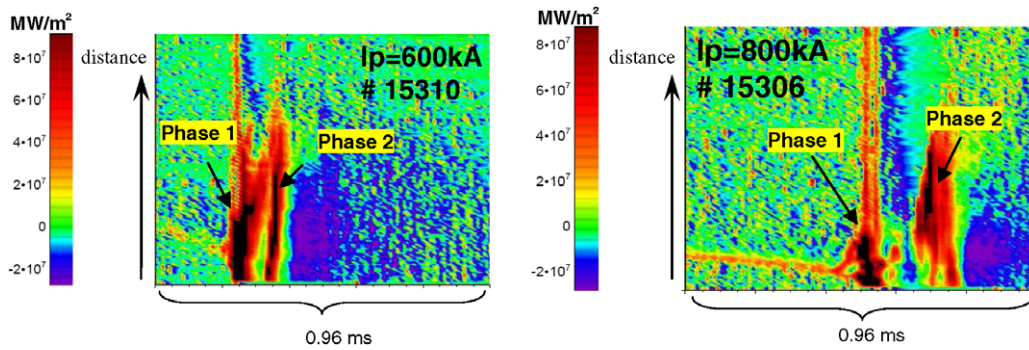


Fig. 6. Flux along divertor tile for two comparable plasma discharges (density and energy stored) for $I_p = 600$ kA (left) and $I_p = 800$ kA (right).

3. Conclusions

Plasma instability in the phase prior to the thermal quench are responsible for the wide range of shape observed on the divertor. MAST gives promising tools to investigate the energy balance, the heat load pattern and the nature of fast transient events. Fast IR measurement and visible images have given clues to better understand the duration and the successive phases appearing during VDE disruptions. Broadening of power width is characteristic of the instability which give rise to the collapse of the plasma: spiral structure for LM and sawtooth triggered disruption and apparent Gaussian radial expansion for VDE disruption. Heat load broadening can varies from 4 to 10 and two main phases can be distinguished. The energy balance between the two phases and the broadening seems to depends on plasma parameters such as I_p and the position of $q = 1$ in the plasma. Further experiments need to be carried in H-mode to deeper investigate the

nature or the broadening (ergodisation and/or spiral structure).

Acknowledgements

This work is jointly funded by Euratom and the United Kingdom Engineering and Physical Sciences Research Council. Dr Delchambre would also like to acknowledge a Euratom Training Fellowship Grant. We also like to thank Geoffrey Cunningham for the fruitful discussions.

References

- [1] A. Loarte et al., IAEA-CN-116/IT/P3-34.
- [2] E. Delchambre et al., PPCF, submitted for publication.
- [3] E. Delchambre, thesis.
- [4] G. Counsell et al., to be published.
- [5] R.J. Buttery et al., Nucl. Fusion 36 (10) (1996).
- [6] A.R. Field et al., in: EX/P2-11, 20th IAEA Fusion Energy Conference, 1–6 November 2004, Vilamoura, Portugal.